Development of a Multicell Methodology to Account for Heterogeneous Core Effects in the Core-Analysis Diffusion Code

Wei Shen*
Atomic Energy of Canada Limited
2251 Speakman Drive, Mississauga, Ontario, Canada L5K 1B2

Abstract

In CANDU® reactor calculations, the lattice-cell cross sections are calculated with WIMS-AECL, and the three-dimensional core neutron-flux and power distributions are calculated with RFSP-IST. The lattice-cell cross sections employed in RFSP-IST and in many other commercial core-analysis diffusion codes are usually based on the use of single-lattice-cell calculations, without considering the effects of the environment. This approximation is not sufficiently accurate for heterogeneous core configurations in the ACR-1000™ . A multicell correction method is therefore developed in RFSP-IST to account for heterogeneous core effects in the design and analysis of ACR-1000. The calculation results show that the multicell methodology developed in RFSP-IST is effective, generic, and it works well for ACR core analysis.

KEYWORDS: CANDU, WIMS-AECL, DRAGON, RFSP-IST, Multicell Method, Lattice-Cell Cross Sections

1. Introduction

In CANDU reactor calculations, the lattice-cell cross sections are calculated with the neutron-transport-code WIMS-AECL [1], and the three-dimensional (3-D) core neutron flux and power distributions are calculated with the neutron-diffusion-code RFSP-IST [2]. The lattice-cell cross sections employed in RFSP-IST and in many other commercial core-analysis diffusion codes are usually based on the use of single-lattice-cell calculations, without considering the effects of the environment. A fundamental assumption in such calculations is that the in-core environment seen by the lattice cell is not greatly different from that of an infinite array of identical lattice cells, so that the single-lattice-cell-based cross sections are valid for core modelling. This fundamental assumption is not sufficiently accurate for certain heterogeneous core configurations which may occur in the ACR-1000, such as checkerboard voiding, and the core-reflector interface. In such scenarios, the adjacent channels will experience significant spectrum interaction, which cannot be addressed by infinite-lattice neutron-transport calculations. The development of a practical model in RFSP-IST to account for the effects of the environment is therefore required in the design and analysis of the ACR-1000.

* Tel. 905-823-9060, Fax. 905-822-0567, E-mail: shenwei@aecl.ca

2. Evaluation of Single-Lattice-Cell Approximation with DRAGON and WIMS-AECL Multicell Models

2.1 ACR Checkerboard Voiding

In the postulated event of a large loss-of-coolant accident (LOCA) in the ACR, the critical pass will void more quickly than the non-critical pass (although the non-critical pass will eventually also void). In the most extreme assumption (not physically possible), half the channels in a core loop are instantly (within a couple of seconds) fully voided, while the other half retain their nominal coolant density. This is referred to as full checkerboard voiding.

To demonstrate the errors associated with the application of single-lattice-cell-based cross sections to ACR checkerboard-voiding scenarios, DRAGON [3] multi-group neutron-transport calculations were performed for an early version of the ACR lattice and fuel (fuel "option-1") with a 2x2 checkerboard multicell model (shown in Figure 1). WIMS-AECL was not used in those calculations, because the versions of WIMS-AECL available at the time (WIMS-AECL version 2.5d and 2.6a) were unable to handle CANDU or ACR multi-cluster geometries when these analyses were performed. The DRAGON multicell results with heterogeneous fuel-burnup or coolant-density distributions were then compared with the results calculated with the DRAGON single-lattice-cell model (shown in Figure 2). The differences in lattice-cell cross sections and k-infinity between the DRAGON single-lattice-cell and multicell results for the cell of interest (herein referred to as Cell-1) are summarized in Table 1.

The comparison shows that the effects of the fuel burnup in the neighbour lattice cells (herein referred to as Cell-2) on the lattice-cell cross sections and k-infinity for Cell-1 is small: the maximum relative difference in the k-infinity for Cell-1 is -0.19% (about 1.5 mk) when discharge-burnup fuel is adjacent to fresh fuel in a checkerboard pattern. The effects of the coolant-density in Cell-2 on the lattice-cell cross sections and k-infinity for Cell-1 is more significant. Use of the conventional single-lattice-cell model without considering heterogeneous coolant-density effects would overestimate the lattice-cell k-infinity for Cell-1 as much as 0.62% (about 6.0 mk) when Cell-1 is voided while Cell-2 remains cooled. This indicates it is necessary to account for heterogeneous coolant-density effects on the lattice-cell cross sections in RFSP-IST for the analysis of ACR checkerboard-voiding scenarios.

2.2 ACR Core-Reflector Interface

Recently, a new capability to handle general multi-cluster geometries with the collision probability method has been developed at AECL in WIMS-AECL version 3 (herein referred to as WIMS-AECL). WIMS-AECL multi-group neutron-transport calculations were performed for an early version of the ACR lattice and fuel (fuel "option-2") with a 5x1 multicell model (shown in Figure 3) to evaluate the accuracy of the single-lattice-cell approximation for the core-reflector interface in the ACR-1000 under nominal operating conditions. The WIMS-AECL multicell results were then compared with the results calculated with the WIMS-AECL single-lattice-cell model (shown in Figure 2). The differences in lattice-cell cross sections and k-infinity for Cell-1 between the WIMS-AECL single-lattice-cell and multicell results are summarized in Table 2.

The comparison shows that the effects of the reflector on the lattice-cell cross sections and k-infinity for the fuel at the core periphery is significant. Use of the conventional single-lattice-cell model without considering the effects of the reflector would overestimate the lattice k-

infinity for Cell-1 by 0.45% (about 3.9 mk), 0.55% (about 5.2 mk), and 0.63% (about 6.2 mk) for fresh, mid-burnup, and discharge-burnup fuel respectively. The comparison also shows that use of the conventional single-lattice-cell model without considering the effects of the environment would significantly underestimate the down-scattering cross section of the reflector by more than 30%. This indicates it is necessary to account for the effects of the environment on the lattice-cell cross sections in RFSP-IST for the modelling of the ACR-1000 core-reflector interface.

3. Development of a Multicell Correction Method in RFSP-IST

Since the traditional assembly discontinuity factor derived from the single-lattice-cell model cannot capture the effects of the environment, several approaches [4-6] have been reported to account for heterogeneous core effects in a Light Water Reactor (LWR) containing both UO_2 and MOX fuels. These approaches use single-lattice-cell calculations for simplicity, and either introduce space-dependent spectral corrections to lattice-cell cross sections obtained from single-lattice-cell calculations, or introduce albedos in single-lattice-cell calculations as corrections to account for local-spectrum effects. Although these approaches seem to work for the LWR core containing both UO_2 and MOX fuels, it was decided not to adopt them in RFSP-IST because in these approaches the lattice-cell cross sections are either corrected based on a case-dependent empirical spectral correction or potentially diverge from the fundamental-mode results when albedos are used in single-lattice-cell calculations.

A straightforward way to capture the effects of the environment on lattice-cell cross sections in RFSP-IST is to generate the lattice-cell cross sections directly from WIMS-AECL multicell neutron-transport calculations for fuels in different regions and under different local and neighbouring conditions. However, this is currently impractical for engineering applications, because of the very large number of WIMS-AECL multicell neutron-transport calculations required to account for local conditions and the burnup history of the fuel, as well as the effects of the environment. A multicell correction method was therefore developed to account for the effects of the environment in RFSP-IST in two steps, as follows:

- Step 1: Cross-section look-up tables (such as the WIMS grid-based tables and/or micro-depletion tables) are generated from extensive WIMS-AECL single-lattice-cell neutron-transport calculations, and these cross-section look-up tables are used in RFSP-IST to generate lattice-cell cross sections with either the WIMS grid-based method [7] or the micro-depletion method [8], according to local conditions and the burnup history of the fuel (as was previously done), and
- Step 2: Heterogeneity factors, generated from WIMS-AECL multicell neutron-transport calculations for some typical cases, are then used in RFSP-IST to introduce corrections to lattice-cell cross sections generated in Step 1 to account for the effects of the environment, as follows:

$$\Sigma_x = \Sigma_x^{\text{single-cell}} \times het\_factor_{\ x} \tag{1}$$

where

Σ_x is the lattice-cell cross section of type x after correction,

$\Sigma_x^{\text{single-cell}}$ is the reference lattice-cell cross section of type x generated with the WIMS-

AECL single-lattice-cell-based model, and

het_factor_x is the heterogeneity factor to be applied to the reference lattice-cell cross sections of type x to account for the effects of the environment.

Compared with other approaches developed to account for heterogeneous core effects in the LWR core containing both UO_2 and MOX fuels, the multicell correction method developed in RFSP-IST is simple and effective, it has fewer approximations and is applicable to any fuel type or heterogeneity scenario considered.

4. RFSP-IST Full-Core Results

4.1 ACR Checkerboard Voiding

To evaluate the validity of the multicell correction method developed in RFSP-IST for the ACR checkerboard-voiding scenarios, preliminary analyses of three hypothetical loss-of-coolant-accident (LOCA) transients in ACR cores (with various types of ACR lattices and fuels) were performed with the kinetics module *CERBERUS of RFSP-IST (first without, and then with the multicell correction superimposed on the WIMS grid-based method). RFSP-IST results were then compared with MCNP [9] full-core results. MCNP and RFSP-IST calculations were performed for selected time steps in the LOCA transients without crediting any action of the shutdown systems. The time-dependent coolant-density distribution was generated from a thermal-hydraulics calculation. Since there is no kinetics model in MCNP, the kinetics module *CERBERUS of RFSP-IST was run in steady-state mode to match the MCNP simulation for each snapshot of the transients. More than 30 million active particle histories were used for each MCNP calculation of the LOCA transients. MCNP and RFSP-IST results (without and with the multicell correction) are plotted in Figure 4. The error bars on the MCNP results correspond to a one-sigma statistical uncertainty.

The results show that, without using the multicell correction model, RFSP-IST- and MCNP-calculated static reactivity changes are initially close but, as the transient develops, the difference in coolant density between neighbouring channels increases and a 1.5-mk difference emerges between RFSP-IST and MCNP results, with the MCNP reactivity being more positive. With the multicell correction on coolant density, the differences in static reactivity change between RFSP-IST and MCNP decrease from 1.5 mk to less than 0.5 mk for most snapshot configurations in the transients. The results also indicate that the multicell correction on fuel burnup is less important than the multicell correction on coolant density for the ACR checkerboard voiding scenarios. It appears that the multicell correction method is effective, and that it produces results that are in good agreement with MCNP snapshot calculations for ACR LOCA transient. It is also worth to note that the multicell correction method developed in RFSP-IST is generic and it is not dependent on the fuel types or the heterogeneity scenarios considered. Even though the comparison was made between RFSP and MCNP for three LOCA transients with three types of ACR lattices and fuels, there is no reason to expect that the multicell correction method would be degraded in other heterogeneity scenarios or for other fuel designs.

4.2 ACR Core-Reflector Interface

To evaluate the influence of the multicell correction method developed in RFSP-IST for the ACR-1000 core-reflector interface under nominal operating conditions, two RFSP-IST calculations were carried out with the static module *SIMULATE of RFSP (first without, and

then with the multicell correction superimposed on the micro-depletion method) for a typical snapshot of an ACR-1000 core. Figures 5 and 6 show the changes induced in the RFSP-IST-calculated channel-power distributions, when the multicell correction method is used. The results show that use of the conventional WIMS-AECL single-lattice-cell model for the core-reflector interface without considering the effects of the environment would underestimate the channel power in the core interior by about 5% and overestimate the channel power at the core periphery by about 5% to 7%. This indicates that it is necessary to use the multicell correction method in RFSP to account for the effects of the environment for the ACR-1000 core-reflector interface.

5. Conclusion

A multicell correction method has been developed and implemented in the CANDU core-analysis diffusion-code RFSP-IST to account for the effects of the environment on the lattice-cell cross sections for the ACR-1000 checkerboard-voiding scenarios at transient conditions and for the ACR-1000 core-reflector interface under nominal operating conditions.

The validity of the multicell correction method for the ACR checkerboard-voiding scenarios was evaluated by comparing the RFSP-IST results (without and with the multicell correction) with MCNP full-core results for three hypothetical LOCA transients in the ACR cores with various types of ACR lattices and fuels. The influence of the multicell correction method for the ACR-1000 core-reflector interface was also assessed by comparing the RFSP-IST results with and without using the multicell correction method for a typical snapshot configuration in an ACR-1000 core. The calculation results show that the multicell methodology developed in RFSP-IST is effective, generic, and it works well for ACR core analysis.

Acknowledgments

The author would like to thank D. Altiparmakov for the development of multi-cluster geometries in WIMS-AECL. Thanks are also due to A. Connolly and D.A. Jenkins who performed MCNP full-core calculations for benchmarking, and to J. Mao who performed RFSP-IST full-core calculations reported in this paper.

References

1. J.D. Irish and S.R. Douglas, “Validation of WIMS-IST”, Proceedings of the 23rd Annual Conference of the Canadian Nuclear Society, Toronto, Ontario, Canada, June 2-5 (2002).
2. B. Rouben, “RFSP-IST, The Industry Standard Tool Computer Program for CANDU Reactor Core Design and Analysis”, Proceedings of the 13th Pacific Basin Nuclear Conference, Shenzhen, China, October 21-25 (2002).
3. G. Marleau, A. Hébert and R. Roy, “A User’s Guide for DRAGON Version DRAGON_000331 Release 3.04”, Report IGE-174, Rev. 5, École Polytechnique de Montréal, 2000 April.
4. Y.A. Chao, Y.A. Shatilla, et al., “Challenges to Nodal Diffusion Methods for Cores with Mixed Oxide Fuel”, Proceedings of the International Conference on the Physics of Nuclear Science and Technology, Long Island, NY, USA, October 5-8 (1998).
5. S. Palmtag and K. Smith, “Two-Group Spectral Corrections for MOX Calculations”,

Proceedings of the International Conference on the Physics of Nuclear Science and Technology, Long Island, NY, USA, October 5-8 (1998).
6. K.T. Clarno and M.L. Adams, "Capturing the Effects of Unlike Neighbors in Single-Assembly Calculations", Nuclear Science and Engineering, **149**, 182 (2005).
7. W. Shen, "Recent Progress in the Development of Cross-Section Models in the Reactor Fuelling Simulation Program (RFSP)", Proceedings of the Mathematics and Computation, Supercomputing, Reactor Physics and Nuclear and Biological Applications, Palais des Papes, Avignon, France, September 12-15 (2005).
8. W. Shen, "Development of a Micro-Depletion Model to Use WIMS Properties in History-Based Local-Parameter Calculations in RFSP", Proceedings of the Sixth International Conference on Simulation Methods in Nuclear Engineering, Montreal, Quebec, Canada, October 13 – 15 (2004).
9. "MCNP4C Monte Carlo N-Particle Transport Code System", Oak Ridge National Laboratory RSICC Computer Code Collection CCC-700, April (2000).

Figure 1: DRAGON/WIMS-AECL 2x2 Checkerboard Multicell Geometry Model

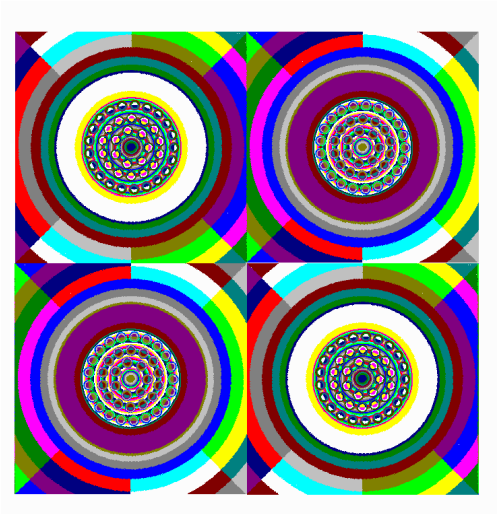

Figure 2: DRAGON/WIMS-AECL Single-Lattice-Cell Geometry Model

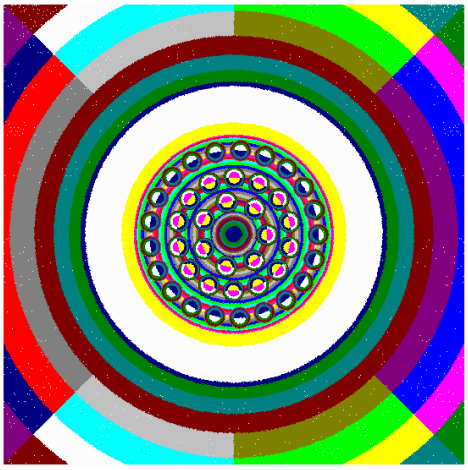

Figure 3: WIMS-AECL 5x1 Core-Reflector Interface Multicell Geometry Model

Figure 4: Comparisons of RFSP-IST and MCNP-Calculated Static Reactivity Changes at Snapshots in Different Hypothetical LOCA Transients in ACR Cores with Various Types of ACR Lattices and Fuels (Without Crediting Any Action of the Shutdown Systems)

30% RIH* Break for an Early Version of the ACR Lattice and Fuel (Fuel "Option-1" without Creep*)

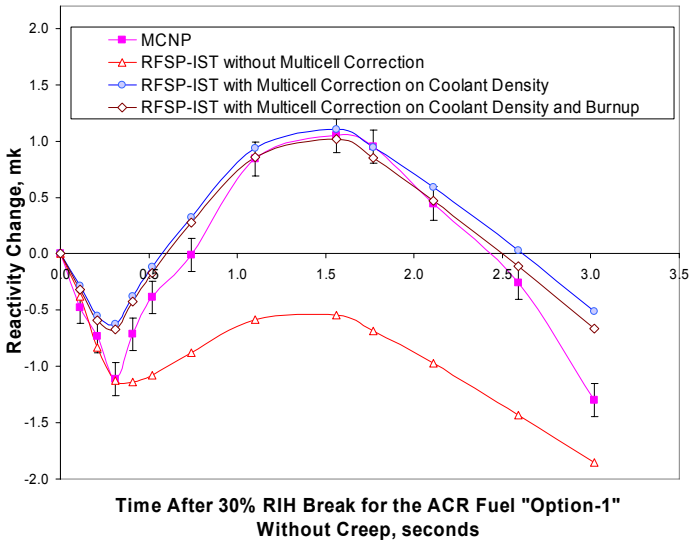

100% ROH* Break for an Early Version of the ACR Lattice and Fuel (Fuel "Option-3" without Creep*)

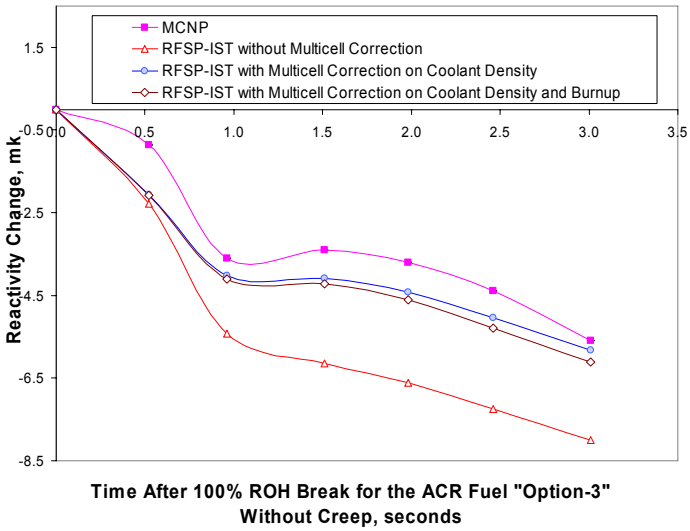

100% ROH* Break for an Early Version of the ACR Lattice and Fuel (Fuel "Option-2" with Creep*)

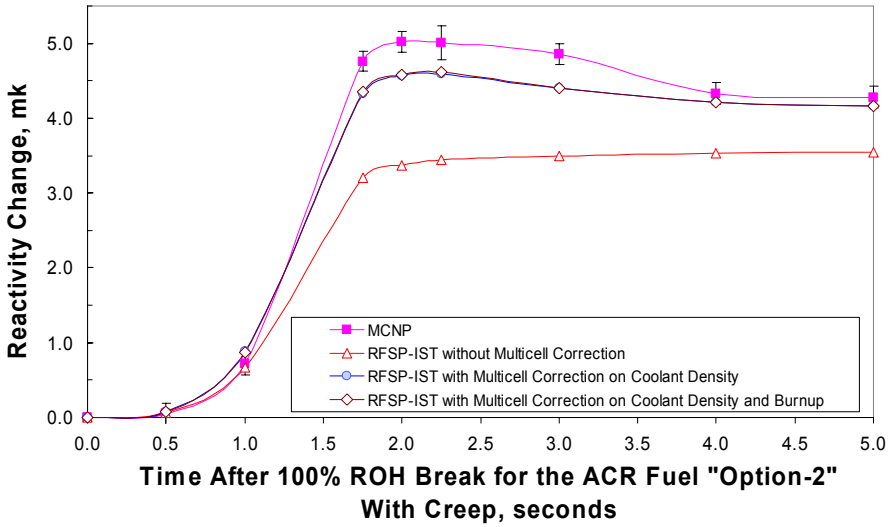

* ROH stands for Reactor Outlet Header; RIH stands for Reactor Inlet Header; Creep is pressure-tube radial growth.

Figure 5: Changes (in %) Induced in the RFSP-IST-Calculated Channel-Power Distributions for an ACR-1000 Core with the Multicell Correction Method

	1	2	3	4	5	6	7	8	9	10	11	12	13	14	15	16	17	18	19	20	21	22	23	24	25	26
A											-4.7	-5.6	-5.6	-5.6	-5.6	-4.7										
B								-4.2	-5.0	-5.2	-6.2	-6.6	-6.6	-6.6	-6.6	-6.2	-5.2	-5.0	-4.2							
C							-3.7	-5.5	-5.8	-5.7	-2.7	-2.5	-2.5	-2.5	-2.5	-2.7	-5.7	-5.8	-5.5	-3.7						
D						-3.3	-4.8	-2.1	-1.8	-1.5	-1.2	-0.9	-0.8	-0.8	-0.9	-1.2	-1.5	-1.8	-2.1	-4.8	-3.3					
E				-3.0	-4.0	-4.6	-1.5	-0.8	-0.4	-0.1	0.1	0.3	0.4	0.4	0.3	0.1	-0.1	-0.4	-0.8	-1.5	-4.6	-4.0	-3.0			
F				-3.8	-4.8	-1.3	-0.5	0.2	0.6	1.0	1.2	1.4	1.5	1.5	1.4	1.2	1.0	0.6	0.2	-0.5	-1.3	-4.8	-3.8			
G			-3.4	-4.6	-1.4	-0.4	0.4	1.0	1.5	1.9	2.2	2.4	2.5	2.5	2.4	2.2	1.9	1.5	1.0	0.4	-0.4	-1.4	-4.6	-3.4		
H		-3.5	-5.0	-1.8	-0.6	0.3	1.1	1.7	2.3	2.7	3.0	3.2	3.3	3.3	3.2	3.0	2.7	2.3	1.7	1.0	0.3	-0.6	-1.8	-5.0	-3.5	
J		-4.3	-5.2	-1.4	-0.1	0.8	1.6	2.3	2.9	3.3	3.7	3.9	4.0	4.0	3.9	3.7	3.3	2.9	2.3	1.6	0.8	-0.1	-1.4	-5.3	-4.3	
K		-4.4	-5.0	-1.0	0.3	1.3	2.1	2.8	3.4	3.8	4.2	4.4	4.5	4.5	4.4	4.2	3.8	3.4	2.8	2.1	1.3	0.3	-1.0	-5.0	-4.4	
L	-3.8	-5.4	-2.0	-0.5	0.6	1.6	2.4	3.1	3.7	4.2	4.6	4.8	4.9	4.9	4.8	4.6	4.2	3.7	3.1	2.4	1.6	0.6	-0.6	-2.0	-5.4	-3.8
M	-4.6	-5.7	-1.8	-0.3	0.8	1.8	2.6	3.4	4.0	4.5	4.8	5.1	5.2	5.2	5.1	4.8	4.5	4.0	3.4	2.6	1.8	0.8	-0.3	-1.8	-5.7	-4.6
N	-4.7	-5.7	-1.7	-0.2	0.9	1.9	2.8	3.5	4.1	4.6	5.0	5.2	5.3	5.3	5.2	5.0	4.6	4.1	3.5	2.8	1.9	0.9	-0.2	-1.7	-5.7	-4.7
O	-4.7	-5.7	-1.7	-0.2	0.9	1.9	2.8	3.5	4.1	4.6	5.0	5.2	5.3	5.3	5.2	5.0	4.6	4.1	3.5	2.8	1.9	0.9	-0.2	-1.7	-5.7	-4.7
P	-4.6	-5.7	-1.8	-0.3	0.8	1.8	2.6	3.4	4.0	4.5	4.8	5.1	5.2	5.2	5.1	4.8	4.5	4.0	3.4	2.6	1.8	0.8	-0.3	-1.8	-5.7	-4.6
Q	-3.8	-5.4	-2.0	-0.6	0.6	1.6	2.4	3.1	3.7	4.2	4.6	4.8	4.9	4.9	4.8	4.6	4.2	3.7	3.1	2.4	1.6	0.6	-0.6	-2.0	-5.4	-3.8
R		-4.4	-5.0	-1.0	0.3	1.3	2.1	2.8	3.4	3.8	4.2	4.4	4.5	4.5	4.4	4.2	3.8	3.4	2.8	2.1	1.3	0.3	-1.0	-5.0	-4.4	
S		-4.3	-5.2	-1.4	-0.1	0.8	1.6	2.3	2.9	3.3	3.6	3.9	4.0	4.0	3.9	3.6	3.3	2.9	2.3	1.6	0.8	-0.1	-1.4	-5.3	-4.3	
T		-3.5	-5.0	-1.8	-0.6	0.3	1.0	1.7	2.3	2.7	3.0	3.2	3.3	3.3	3.2	3.0	2.7	2.2	1.7	1.0	0.3	-0.6	-1.8	-5.0	-3.5	
U			-3.4	-4.6	-1.4	-0.4	0.4	1.0	1.5	1.9	2.2	2.4	2.5	2.5	2.4	2.2	1.9	1.5	1.0	0.3	-0.4	-1.4	-4.6	-3.4		
V				-3.8	-4.8	-1.3	-0.5	0.2	0.6	1.0	1.2	1.4	1.5	1.5	1.4	1.2	1.0	0.6	0.1	-0.5	-1.4	-4.8	-3.8			
W				-3.0	-4.0	-4.6	-1.5	-0.8	-0.4	-0.1	0.1	0.3	0.4	0.4	0.3	0.1	-0.1	-0.4	-0.8	-1.5	-4.6	-4.0	-3.0			
X						-3.3	-4.8	-2.1	-1.8	-1.5	-1.2	-0.9	-0.9	-0.9	-0.9	-1.2	-1.5	-1.8	-2.1	-4.8	-3.3					
Y							-3.7	-5.5	-5.8	-5.7	-2.7	-2.5	-2.5	-2.5	-2.5	-2.7	-5.7	-5.9	-5.5	-3.8						
Z								-4.2	-5.0	-5.2	-6.2	-6.6	-6.6	-6.6	-6.6	-6.2	-5.2	-5.0	-4.2							
ZZ											-4.7	-5.6	-5.7	-5.7	-5.6	-4.7										

Figure 6: RFSP-IST-Calculated Channel-Power Distributions for an ACR-1000 Core with and without the Multicell Correction Method

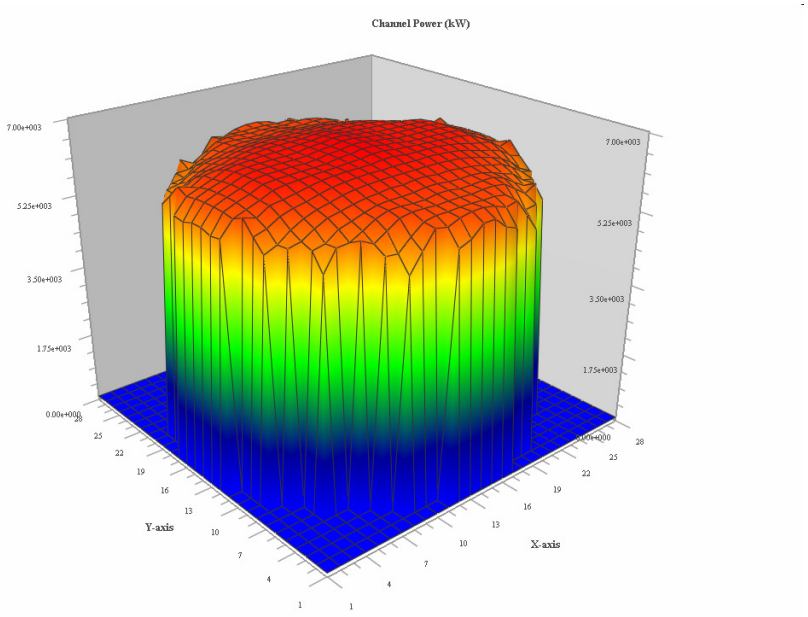

Without Multicell Correction

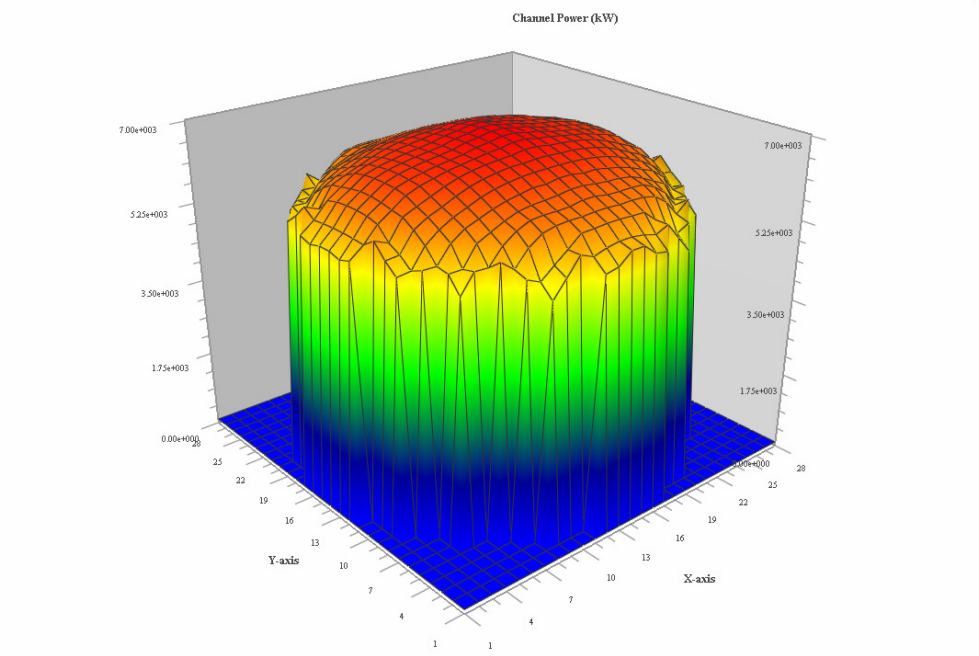

With Multicell Correction

Table 1: Differences in Lattice-Cell Cross Sections[1] and K-Infinity Between the DRAGON Multicell and Single-Lattice-Cell Results for ACR[2] Checkerboard Voiding Scenarios

Fuel Burnup		Coolant Density		Differences: $\varepsilon(\Sigma_x)=100\times\left(\Sigma_x^{multicell}-\Sigma_x^{single-cell}\right)/\Sigma_x^{single-cell}$ & $\varepsilon(k_\infty)=100\times\left(k_\infty^{multicell}-k_\infty^{single-cell}\right)/k_\infty^{single-cell}$									
Cell-1	Cell-2	Cell-1	Cell-2	Σ_{a1}	Σ_{a2}	$\Sigma_{s1\to2}$	$\Sigma_{s2\to1}$	Σ_{tr1}	Σ_{tr2}	$\nu\Sigma_{f1}$	$\nu\Sigma_{f2}$	F	K_∞
fresh	discharge	cooled		0.49	0.31	-2.93	0.77	-0.32	0.08	3.16	0.30	-0.52	-0.19
discharge	fresh			-0.16	-0.32	3.15	-0.79	0.33	-0.08	-5.29	-0.34	0.55	0.02
fresh	discharge	voided		-0.58	0.14	-3.31	-0.34	-0.57	0.13	2.10	0.16	0.63	-0.01
discharge	fresh			0.87	-0.03	3.48	0.46	0.60	-0.12	-4.36	0.04	-0.71	-0.16
fresh		cooled	voided	0.30	2.70	2.17	18.68	0.49	-0.20	-2.74	2.64	-0.47	-0.19
		voided	cooled	-2.02	1.12	-3.16	-16.46	-0.83	0.88	1.91	1.24	3.89	0.62
mid-burnup		cooled	voided	0.48	3.19	1.79	18.39	0.47	-0.20	-3.55	3.48	-0.06	-0.04
		voided	cooled	-2.02	0.41	-2.62	-16.18	-0.81	0.79	3.17	0.24	3.46	0.62
discharge		voided	cooled	0.44	3.31	1.33	19.82	0.46	-0.24	-4.53	3.88	-1.02	0.08
		voided	cooled	-1.79	0.25	-2.26	-17.26	-0.78	0.81	4.58	-0.14	4.33	0.55

Table 2: Differences in Lattice-Cell Cross Sections and K-Infinity Between the WIMS-AECL Multicell and Single-Lattice-Cell Results for ACR[3] Core-Reflector Interface

Core-Reflector Interface	Fuel Burnup	Differences: $\varepsilon(\Sigma_x)=100\times\left(\Sigma_x^{multicell}-\Sigma_x^{single-cell}\right)/\Sigma_x^{single-cell}$ & $\varepsilon(k_\infty)=100\times\left(k_\infty^{multicell}-k_\infty^{single-cell}\right)/k_\infty^{single-cell}$											
		Σ_{a1}	Σ_{a2}	$\Sigma_{s1\to2}$	$\Sigma_{s2\to1}$	Σ_{tr1}	Σ_{tr2}	$\nu\Sigma_{f1}$	$\nu\Sigma_{f2}$	F	H1	H2	K_∞
Fuel at the Core Periphery	fresh	1.36	-2.62	-6.88	-18.10	-1.14	0.47	5.43	-2.46	-3.76	4.94	-2.46	-0.45
	mid-burnup	1.16	-2.89	-6.88	-18.55	-1.14	0.49	6.01	-2.92	-3.75	5.58	-2.88	-0.55
	discharge	0.98	-2.91	-6.90	-18.61	-1.14	0.49	6.62	-3.06	-3.62	6.25	-3.01	-0.63
Reflector	fresh	-3.24	1.73	32.49	-51.84	1.28	0.82	-	-	-	-	-	-
	mid-burnup	-2.78	1.47	29.99	-47.83	1.19	0.69	-	-	-	-	-	-
	discharge	-2.42	1.23	28.13	-43.73	1.13	0.57	-	-	-	-	-	-

[1] F refers to the F factor which is the ratio of fuel-average to cell-average thermal neutron flux (dimensionless), H refers to the H factor which is the energy produced from each energy group (kW/bundle/(10^{11}n/cm^2/s)), the subscripts 1 and 2 refer to the fast and thermal group respectively, and the other quantities are the conventionally-used cross-section symbols.

[2] Calculations were performed on an early version of ACR lattice and fuel (fuel "option-1").

[3] Calculations were performed on an early version of ACR lattice and fuel (fuel "option-2").